

Bent-core dopant in a liquid crystal having a reentrant synclincic phase

Min Hua Zhu and Charles Rosenblatt*

Department of Physics, Case Western Reserve University, Cleveland, Ohio 44106, USA

Julie M. Kim and Mary E. Neubert

Liquid Crystal Institute, Kent State University, Kent, Ohio 44242, USA

(Received 20 May 2004; published 14 September 2004)

Small quantities of the bent-core mesogen P-7PIMB were dissolved in an anticlinic liquid crystal consisting of a mixture of left- and right-handed TFMHPOBC, with enantiomer excess $X=0.2$. The bent-core dopant promotes anticlinic order at higher temperatures, but becomes less effective in suppressing the synclincic phase at the reentrant synclincic transition due to an orientational transition of the dopant within the calamitic TFMHPOBC matrix. Measurements of the anticlinic-synclincic electric-field switching threshold as a function of temperature and dopant concentration facilitate a determination of the component of the anticlinic interaction coefficient U that is due to the bent-core dopant. It is found that the value of U per bent-core molecule is much larger than the corresponding value for a pair of TFMHPOBC molecules in adjacent smectic layers.

DOI: 10.1103/PhysRevE.70.031702

PACS number(s): 61.30.Gd

Several recent studies have examined the effect of bent-core dopant molecules—these are sometimes known as “banana” or “bowshaped”—that are dissolved in a calamitic liquid crystal matrix [1–6]. In particular, Gorecka *et al.* studied the behavior of a mixture of bent-core molecules dissolved in a liquid crystal that has a synclincic smectic- C^* ($Sm-C^*$) phase [5]. Here the asterisk denotes that the molecule is chiral. The bent-core mesogens were found to promote anticlinic smectic- C_A^* ($Sm-C_A^*$) order, as the bent-core symmetry axis lies parallel to the interface between adjacent smectic layers, and the bent-core plane lies parallel to the tilt plane of the anticlinic phase. For a sufficiently large bent-core concentration, the synclincic phase disappears and a direct isotropic-to-anticlinic phase transition was observed. More recently we demonstrated a combined orientational-positional transition of the bent-core mesogen in the anticlinic $Sm-C_A^*$ phase when its concentration $C \geq 3$ wt%: Above this concentration the bent-core mesogen resides approximately within a single smectic layer with its symmetry axis parallel to the local calamitic tilt axis in that layer [6].

Concomitant with this work have been investigations of reentrant behavior in enantiomeric mixtures of liquid crystals that exhibit an anticlinic phase. Pocięcha *et al.* examined homologs of an anticlinic compound and observed a $Sm-C^*-Sm-C_A^*$ -reentrant $Sm-C^*$ phase sequence with decreasing temperature above a certain homolog number [7]. This phase sequence also has been observed on cooling thin films that are subjected to an applied electric field [8,9]. More recently we examined the electric-field-temperature phase diagram for mixtures of right- and left-handed enantiomers of TFMHPOBC (Fig. 1). We found that for small enantiomer excess X , where $X \equiv ([R]-[S])/([R]+[S])$ and where $[R]$ and $[S]$ denote the mole fractions of right- and left-handed enantiomers, respectively, a reentrant $Sm-C^*$

phase occurs on cooling for sufficiently large electric fields [10]. A simple phenomenological theory that accounts for layer-layer interactions was developed, such that the electric-field-induced transition to the synclincic phase is facilitated by a percolation mechanism, which then propagates via solitary waves.

In this paper we report on experiments that combine these two phenomena, viz., the effects of a bent-core dopant on the behavior of an enantiomeric mixture of calamitic molecules that exhibits a reentrant synclincic phase. Several notable features were observed: The dopant stabilizes the anticlinic phase against electric-field-induced switching into the synclincic phase, similar to the behavior noted by Gorecka *et al.* [5]; the behavior of the temperature T vs electric field E phase transition curves varies regularly with C at the higher temperature $Sm-C^*-Sm-C_A^*$ phase transition; the temperature T_∞ at which $dT/dE \rightarrow \infty$ on the $T-E$ phase diagram increases with increasing dopant concentration C ; and the T vs E curves for the lower temperature reentrant transition exhibit anomalous behavior for dopant concentrations $C \geq 3$ wt%. A detailed analysis of the data facilitates a determination of the component of the anticlinic interaction coefficient U that is associated with the bent-core dopant dissolved in the TFMHPOBC. Here U is the polar-tilt-angle- (θ) -dependent coefficient of the free energy term $F_U = U/2[\cos(\varphi_{i-1}-\varphi_i) + \cos(\varphi_i-\varphi_{i+1})]$ that promotes anticlinic order relative to synclincic order [11], where φ_i is the azimuthal angle of the average molecular orientation in smectic layer i .

Five liquid crystal mixtures were formulated. First, a single batch of TFMHPOBC having enantiomer excess $X=0.2$ was prepared. From this initial batch, five samples were made by dissolving the bent-core molecule P-7PIMB (Fig. 2)

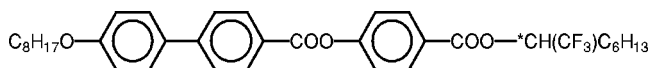


FIG. 1. Structure of TFMHPOBC.

*Author to whom for correspondence should be addressed. Email address: rosenblatt@case.edu

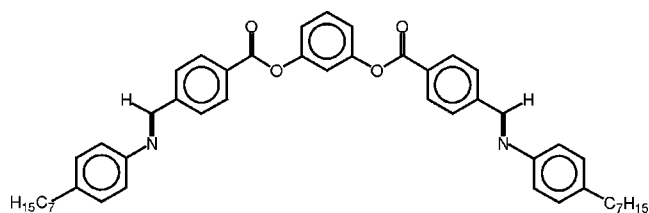


FIG. 2. Structure of bent-core molecule P-7PIMB.

into the TFMHPOBC matrix. The final mixtures had P-7PIMB concentrations $C=0, 1, 2, 3$, and 4 wt %, each with an uncertainty of ± 0.1 wt %. The temperature-concentration phase diagram in the absence of an applied voltage was measured by differential scanning calorimetry [6]; the results for $T > 100^\circ\text{C}$ are shown in Fig. 3. Cells were prepared using two indium-tin-oxide-coated glass slides, which were cleaned and then spin-coated with the polyamic acid RN-1175 (Nissan Chemical Industries). The slides were baked at 250°C for 1 h and then rubbed with a cotton cloth affixed to a rubbing machine. The slides were placed together, separated by strips of Mylar of nominal spacing $5\ \mu\text{m}$, and cemented. (An exception was made for the cell containing the highest concentration $C=4$ because of the very large fields required to switch the sample into the synclincic phase. In this case $2\ \mu\text{m}$ Mylar strips were used.) The cells were placed in a temperature-controlled hot stage, which in turn was placed on a rotation stage, and the thickness d of each cell was determined by an interference technique. The thicknesses of the five cells were found to be $d=8.2, 7.0, 6.9, 6.0$, and $3.4\ \mu\text{m}$ for the $C=0, 1, 2, 3$, and 4 wt % samples, respectively; the uncertainty in d was $\pm 0.1\ \mu\text{m}$. Observations of optical interference patterns indicate that cell thickness variations with temperature were negligible from room temperature up to the highest temperature used in the experiment. Additionally, previous measurements on TFMHPOBC indi-

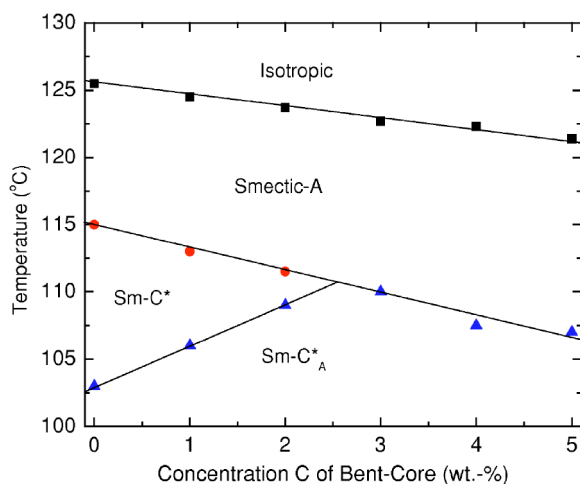


FIG. 3. Concentration-temperature phase diagram for an $X=0.2$ enantiomeric mixture of TFMHPOBC as a function of bent-core concentration C at zero applied field. \blacksquare corresponds to the isotropic to smectic-A transition line, \bullet to the Sm-A–Sm- C^* transition line, and \blacktriangle to the transition into the Sm- C_A^* phase. Lines are drawn as a guide to the eye.

cate that the threshold field E_{th} for switching from the Sm- C_A^* to the Sm- C^* phase is not sensitive to cell thickness [11]. Cells were then filled at $T=130^\circ\text{C}$, corresponding to the isotropic phase of the liquid crystal mixtures, and cooled slowly to ensure good alignment through the smectic-A and synclincic Sm- C^* phases, and then into the anticlinic Sm- C_A^* phase.

Let us briefly address the issue of helicity. Ordinarily, the anticlinic phase is twisted into a double helix, with the azimuthal orientation in each layer approximately 180° out of phase with its neighboring layer [12]. The helical pitch for optically pure ($X=1$) TFMHPOBC varies from approximately 0.6 to $1.0\ \mu\text{m}$ over the temperature range of interest [13]. Thus, for an enantiomeric excess $X=0.2$, we would expect a pitch ranging between $3\ \mu\text{m}$ at lower temperatures and $5\ \mu\text{m}$ at higher temperatures. This pitch is sufficiently long that the helices are likely to be unwound, i.e., in a surface-stabilized state. Although it has been shown that the addition of an achiral bent-core dopant to a chiral calamitic liquid crystal can *decrease* the pitch of the mixture [14], the fractional pitch change tends to be relatively small ($\sim 20\%$) for the relevant concentrations. The apparent absence of pitch lines for our mixtures and the near temperature independence of the absorption spectrum for each concentration C —Ref. [10] shows the $C=0$ absorption spectrum—also indicate that our sample is unwound for all concentrations and temperatures used in this experiment [10].

While viewing the cell under a polarizing microscope, a 1 Hz monopolar square wave voltage was applied to the sample, with the voltage switching between 0 and V every half cycle. The amplitude V of the square wave was ramped slowly upward until fingerlike solitary waves of synclincic phase invading the anticlinic were observed, and the threshold voltage V_{th} was recorded; the threshold field $E_{th}=V_{th}/d$. Measurements at each concentration C were made as a function of temperature on cooling, and the resulting phase diagram T vs E is shown in Fig. 4. We note that, in principle, our $C=0$ wt % data and the data for $X=0.2$ in Ref. [10] should be identical. The threshold fields presented in Fig. 4, however, are approximately 20% larger than those in Ref. [10]. The reasons for this discrepancy lie principally in variations of the thickness of the alignment layers, as well as the accuracy of X when formulating the enantiomeric mixtures of TFMHPOBC: Although the nominal enantiomer excess for both starting mixtures is $X=0.2$, a small difference in X would result in a large shift in E_{th} [10]. A small contribution also may have come from the fact that different polyimides were used for alignment in the two experiments. Nevertheless, in no way do these issues alter our discussion below. Additionally, we remark that the theoretical approach adopted in Ref. [10] is based on a second order percolation of synclincic molecular pairs in adjacent smectic layers. The appearance of solitary waves with a positive velocity above a threshold field E_{th} is due to kinetic effects associated with the percolated synclincic regions, and is analogous to the coalescence of ferromagnetic domains through domain wall propagation on quenching a ferromagnet material below its transition temperature. Thus the measured threshold fields correspond to a positive solitary wave velocity, which must occur above the percolation threshold.

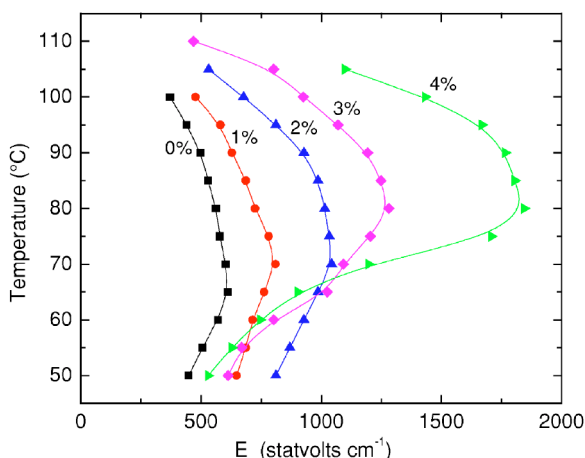


FIG. 4. Electric field–temperature phase diagram at different concentrations C . For a given concentration C , the anticlinic phase is to the left of the curve, the synclinic phase is to the right of the curve, and T_{∞} is the point at which E_{th} is maximum. ■ corresponds to $C=0$ wt % bent-core dopant, ● to $C=1$, ▲ to $C=2$, ◆ to $C=3$, and ► to $C=4$ wt %. The broad bent-core orientational transition, whose differential scanning calorimetry peak is at T_c , occurs in the region $50 < T < 60^{\circ}\text{C}$ for $C=3$ wt % and $60 < T < 70^{\circ}\text{C}$ for $C=4$ wt % mixtures. The uncertainty δE_{th} in the threshold field is $\pm 3\%$. Lines are drawn as a guide to the eye.

Our next task is to obtain the interaction coefficient U , which is equal to $1/2PE_{th}$, where P is the spontaneous polarization associated with the $\text{Sm}-C^*$ phase [11]. In our calculations below, we assume that P is a function of the polar tilt angle θ and enantiomer excess X only, and that corrections to P due to the presence of small concentrations of bent-core dopant, which do not contribute to the polarization [5], are small. We obtain P by assuming that $P=XP_0$, where $X=0.2$ in our experiment and P_0 is the polarization of the optically pure ($X=1$) material. P_0 vs temperature is available in the literature [15], and can be parametrized as $P_0(\theta)$ from our previously published data for the polar tilt angle vs temperature for an optically pure sample of TFMHPOBC [16]. Thus we obtain the polarization $P(\theta)=XP_0(\theta)$ for $X=0.2$ and

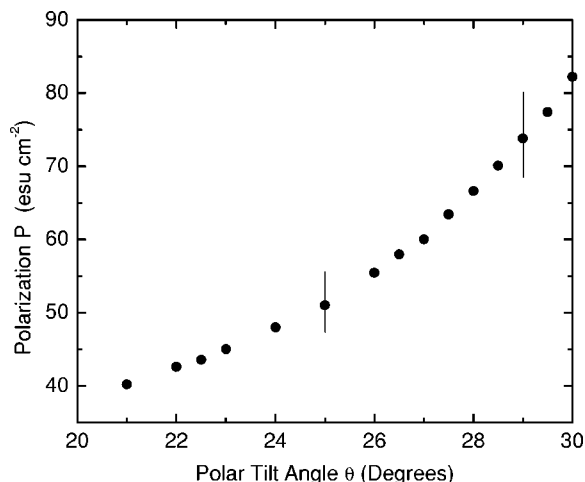


FIG. 5. Calculated polarization P vs polar tilt angle θ .

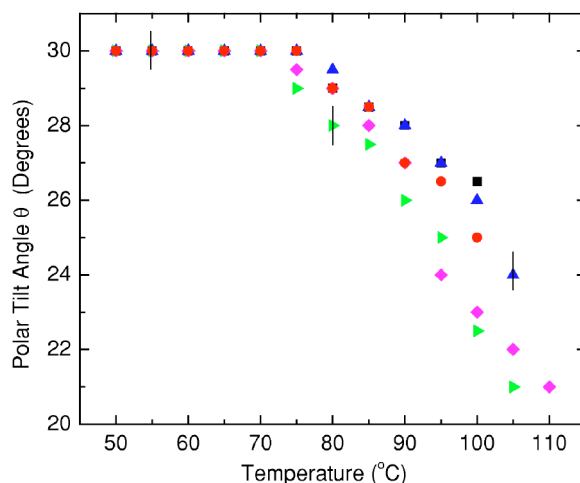


FIG. 6. Polar tilt angle θ vs temperature for five bent-core concentrations. See Fig. 4 caption for symbols.

$C=0$, which is shown in Fig. 5. We then measure the polar tilt angle θ as a function of temperature for each bent-core concentration C . To do so, a dc voltage was applied to switch the cell from anticlinic to synclinic, and the microscope stage was rotated to minimize the transmitted light intensity. This rotation angle corresponds to the polar tilt angle θ , and is shown in Fig. 6. Note that θ apparently saturates at $(30 \pm 0.5)^{\circ}$ for all concentrations. Finally, from the θ vs T data (Fig. 6) and from the P vs θ data (Fig. 5), we obtain P as a function of temperature for each dopant concentration C . We then use these values of P , along with the data in Fig. 4, to determine $U=1/2PE_{th}$ as a function of temperature and dopant concentration; the results are shown in Fig. 7. From Figs. 6 and 7 we can plot U vs. θ , which is shown in Fig. 8.

Several features are immediately apparent. In Fig. 4 we note that at a given temperature $T > T_{\infty}$ the field needed to switch the liquid crystal from the (higher temperature) anti-

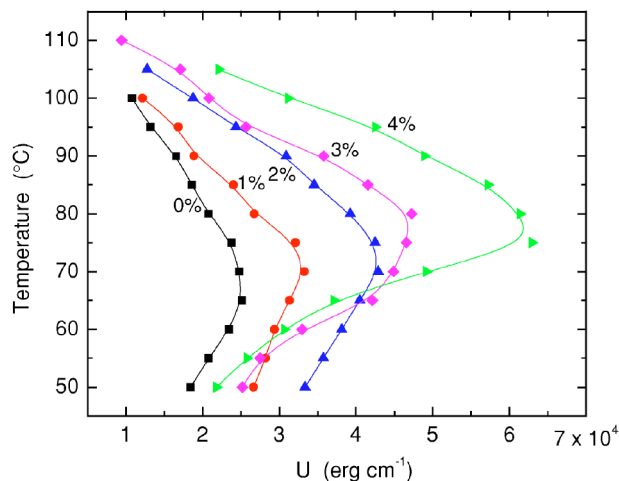


FIG. 7. Temperature vs interaction coefficient U . See Fig.4 caption for symbols. The uncertainty δU derives from uncertainties in E_{th} and in P , and is approximately $\pm 10\%$. Lines are drawn as a guide to the eye.

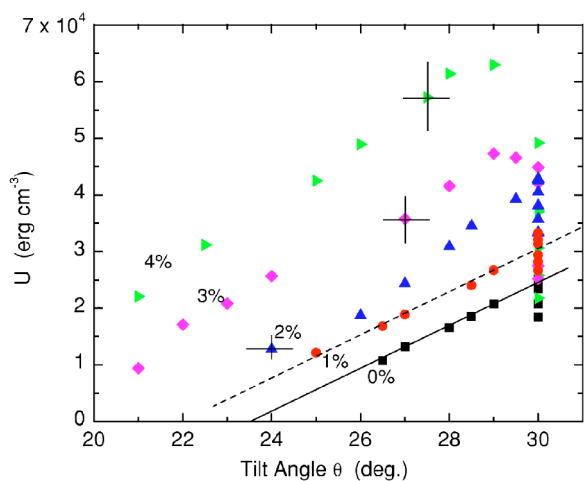


FIG. 8. Interaction coefficient U vs polar tilt angle θ . The solid and dashed lines are linear extrapolations of the $C=0$ and 1 wt % data, respectively. See Fig. 4 caption for symbols.

clinic to the synclinc phase increases with increasing C . Moreover, this field grows faster-than-linearly in C , consistent with the results in Ref. [5]. Additionally, for a fixed applied field, e.g., $750 \text{ statvolt cm}^{-1}$, not only does the $\text{Sm}-C^*-\text{Sm}-C_A^*$ phase transition temperature increase with increasing C —this also was noted in Ref. [5]—but the lower temperature $\text{Sm}-C_A^*-\text{reentrant Sm}-C^*$ transition temperature decreases with increasing C for $C \leq 2$ wt %. Clearly, the anticlinic $\text{Sm}-C_A^*$ phase is becoming more stable with increasing C relative to both the high temperature and reentrant $\text{Sm}-C^*$ phases. Another feature to note is that for $C = 3$ wt %, and even much more so for $C = 4$ wt %, the threshold field E_{th} decreases sharply with temperature for $T < T_\infty$ (that is, at the reentrant transition). This trend is so strong that for a given low temperature, e.g., 50°C , $E_{th}(C=4) < E_{th}(C=3) < E_{th}(C=1)$. The origin of this effect is a thermally broad transition around temperature T_c involving orientational and positional changes of the bent-core dopant for concentrations $C \geq 3$ wt %, which was observed using differential scanning calorimetry and infrared absorption [6]. Above this concentration-dependent bent-core orientational-positional transition temperature T_c , the plane of the bent-core molecule lies parallel to the tilt plane of the anticlinic matrix, with the bent-core symmetry axis parallel to the smectic layers [Figs. 9(a) and 9(b)]. For $T < T_c$ the bent-core molecule reorients and repositions itself so that it lies approximately within a single smectic layer, with the polar tilt of its symmetry axis approximately equal to the polar tilt of the TFMHPOBC molecule and the vector that connects the two ends of the bent-core molecule lying approximately perpendicular to the anticlinic tilt plane [Figs. 9(c) and 9(d)]. With the symmetry axis of the bent-core dopant adopting an orientation parallel to the calamitic molecules within each layer for $T < T_c$, one would expect that the switching threshold would decrease, which is observed experimentally. Additionally, as observed in Ref. [6], T_c increases with increasing concentration C ; this is consistent with the data in Fig. 4, where the sharp change in E_{th} can be associated with the bent-core orientational-positional transition, which occurs at

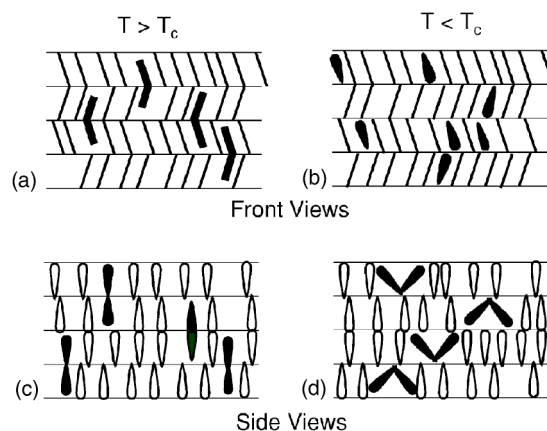


FIG. 9. Schematic representation of molecules. (a) and (b) represent the orientation above the bent-core orientational transition temperature T_c for all concentrations C . In (a) the light lines represent TFMHPOBC and the heavy lines the bent-core P-7PIMB molecules. In (b) the open figures represent TFMHPOBC and the solid figures the bent-core P-7PIMB molecules. (b) shows the side view, as if (a) were viewed from the right. The wider parts of the molecules indicate that those parts are tilted toward the viewer. (c) and (d) show the bent-core orientations below T_c for $C=3$ and 4 wt %. In (c) the light lines represent TFMHPOBC and the heavy lines the bent-core P-7PIMB molecules. In (d) the open figures represent TFMHPOBC and the solid figures the bent-core P-7PIMB molecules.

a higher temperature for $C=4$ than for $C=3$ wt %. Interestingly, with decreasing temperature for $T \leq 60^\circ\text{C}$, the slope dT/dE is larger than it is at higher temperatures, and in fact the T vs E curves for $C=3$ and 4 wt % appear to approach the curve for $C=0$. This would indicate that by $T \sim 50^\circ\text{C}$ the bent-core transition is nearly complete statistically, and the system behaves as if it were a (nearly) pure enantiomeric mixture of TFMHPOBC without the bent-core dopant. Qualitatively the same behavior is also seen in Fig. 7 in the T vs U curves. It is worth noting that other such transitions have been predicted: Numerical simulations of a photoactive solute in a smectic- A host indicate that the dopant is driven to locations between the layers upon photoisomerization from *trans* to *cis* [17].

Let us now turn to Figs. 6 and 8, where we see that the polar tilt angle θ in the anticlinic phase *right at* the $\text{Sm}-C^*-\text{Sm}-C_A^*$ transition temperature is largest for $C=0$ and decreases with increasing dopant concentration. This can be understood from Fig. 3, which shows that the temperature range of the $\text{Sm}-C^*$ phase is widest at $C=0$ and decreases with increasing C , finally vanishing at approximately $C = 3$ wt %. As the $\text{Sm}-A-\text{Sm}-C^*$ transition is second order, the molecular tilt θ at lower bent-core concentrations C has a larger temperature region over which to grow before the onset of the $\text{Sm}-C_A^*$ phase. More significantly, we note from Fig. 8 that for each concentration C , the interaction coefficient U is approximately linear over the limited range of θ until saturation occurs at $\theta \approx 30^\circ$, with the slopes $dU/d\theta$ all approximately equal. Consider a linear extrapolation of the $C=0$ data to $U=0$ at $\theta \approx 23.5^\circ$ (solid line in Fig. 8). A vanishing interaction coefficient U corresponds to an infinite

susceptibility for $\text{Sm}-C^*$ fluctuations within the $\text{Sm}-C_A^*$ phase, i.e., the optic mode becomes infinitely soft. (Although a nonzero polar tilt and the associated dipolar interactions between pairs of TFMHPOBC molecules in adjacent layers tend to promote large values of U , there exists a competing effect: Reduced steric hindrance associated with R and S pairs inhibits anticlinic order and tends to reduce the effective value of U [10].) Relatively noninvasive measurements of U performed by probing the optic mode response to very small electric fields have been shown to be consistent with the much more highly invasive anticlinic-to-synclinc switching method used herein [18]. This indicates that the interaction potential scales quadratically with the azimuthal deviations $|\varphi_{i-1}-\varphi_i|-\pi$, even out to large deviations, and that the single Fourier component form for F_U is physically realistic [18]. Thus, since U extrapolates to zero at $\theta \approx 23.5^\circ$ for $C=0$, the nonzero values of U at $\theta \approx 23.5^\circ$ for $C>0$ can be attributed directly to the presence of the bent-core dopant. We find $U=0.6, 1.2, 2.2$, and $3.7 \times 10^4 \text{ erg cm}^{-3}$ for $C=1, 2, 3$, and 4 wt %, respectively, at $\theta \approx 23.5^\circ$. The uncertainty for each of these values of U is approximately $\pm 10\%$. Although U vs C becomes nonlinear for large C , for small concentrations $U \propto C$ and the presence of the bent-core dopant serves as a stiffening agent against optic mode fluctuations. We can compare the effects on U of the bent-core dopant with the ordinary contributions to anticlinic behavior from pairs of TFMHPOBC molecules in adjacent layers. For a molecular weight 720 for the P-7PIMB dopant and 612 for the TFMHPOBC, and assuming a mass density $\rho=1 \text{ g cm}^{-3}$, we find from $U=0.6 \times 10^4 \text{ erg cm}^{-3}$ at $C=1 \text{ wt } \%$ (when extrapolated to $\theta=23.5^\circ$) that the interac-

tion coefficient of the bulk system per bent-core molecule $u_{P-7PIMB}=7.2 \times 10^{-16} \text{ erg}$. To be sure, $u_{P-7PIMB}$ is not the deformation energy of the bent-core molecule, but rather it represents an energy associated with the anticlinic-to-synclinc transition of the bulk mixture when an additional bent-core molecule is added. We now compare this bent-core molecular interaction coefficient $u_{P-7PIMB}$ with the interaction coefficient $u_{TFMHPOBC}$ for a pair of TFMHPOBC molecules. Because $U=0$ when we extrapolate the data at $C=0$ (no bent-core dopant) to $\theta=23.5^\circ$, we shall estimate $u_{TFMHPOBC}$ at the $\text{Sm}-C^*-\text{Sm}-C_A^*$ transition temperature instead. Here $U=1.1 \times 10^4 \text{ erg cm}^{-3}$ (and $\theta=26.5^\circ$) for $C=0$, and we find $u_{TFMHPOBC}=2.3 \times 10^{-17} \text{ erg}$. It is clear that the bent-core molecule adds considerable stiffness to the mixture.

The results presented herein indicate a number of interesting phenomena regarding bent-core-calamitic mixtures and reentrant behavior, and open the possibility of tailoring the switching behavior of anticlinic devices with small quantities of dopants. Finer control also may be obtained with bimesogenic dopants that are less rigid, although this remains the subject of future study.

ACKNOWLEDGMENT

We thank Dr. Neha M. Patel and Dr. M. Reza Dodge for useful conversations and Dr. Ichiro Kobayashi of Nissan Chemical Industries for providing the RN-1175 polyamic acid. This work was supported by the National Science Foundation's Solid State Chemistry Program under Grant No. DMR-0345109.

-
- [1] R. Pratibha, N. V. Madhusudana, and B. K. Sadashiva, *Science* **288**, 2184 (2000).
- [2] R. Pratibha, N. V. Madhusudana, and B. K. Sadashiva, *Mol. Cryst. Liq. Cryst. Sci. Technol., Sect. A* **365**, 755 (2001).
- [3] R. Pratibha, N. V. Madhusudana, and B. K. Sadashiva, *Pramana* **61**, 405 (2003).
- [4] M. R. Dodge, R. G. Petschek, C. Rosenblatt, M. E. Neubert, and M. E. Walsh, *Phys. Rev. E* **68**, 031703 (2003).
- [5] E. Gorecka, M. Nakata, J. Mieczkowski, Y. Takanishi, K. Ishikawa, J. Watanabe, H. Takezoe, S. H. Eichorn, and T. M. Swager, *Phys. Rev. Lett.* **85**, 2526 (2000).
- [6] M. H. Zhu, M. R. Dodge, T. Shioda, C. Rosenblatt, D. D. Parker, J. M. Kim, and M. E. Neubert, *Liq. Cryst.* (to be published).
- [7] D. Pocięcha, E. Gorecka, M. Cepic, N. Vaupotic, B. Zeks, D. Kardas, and J. Mieczkowski, *Phys. Rev. Lett.* **86**, 3048 (2001).
- [8] C. Y. Chao, C. R. Lo, P. J. Wu, Y. H. Liu, D. R. Link, J. E. Maclennan, N. A. Clark, M. Veum, C. C. Huang, and J. T. Ho, *Phys. Rev. Lett.* **86**, 4048 (2001).
- [9] P. J. Wu, C. Y. Chao, C. R. Lo, M. Veum, D. R. Link, J. E. Maclennan, and N. A. Clark, *Ferroelectrics* **277**, 511 (2002).
- [10] N. M. Patel, C. Rosenblatt, and Y.-K. Yu, *Phys. Rev. E* **68**, 011703 (2003).
- [11] J. F. Li, X.-Y. Wang, E. Kangas, P. L. Taylor, C. Rosenblatt, Y. Suzuki, and P. E. Cladis, *Phys. Rev. B* **52**, R13075 (1995).
- [12] Y. P. Panarin, O. Kalinovskaya, and J. K. Vij, *Liq. Cryst.* **25**, 241 (1998).
- [13] J. Li, H. Takezoe, and A. Fukuda, *Jpn. J. Appl. Phys., Part 1* **30**, 532 (1991).
- [14] E. Gorecka, M. Cepic, J. Mieczkowski, M. Nagata, H. Takezoe, and B. Zeks, *Phys. Rev. E* **67**, 061704 (2003).
- [15] Y. Suzuki, T. Hagiwara, I. Kawamura, N. Okamura, T. Kitazume, M. Kakimoto, Y. Imai, Y. Ouchi, H. Takezoe, and A. Fukuda, *Liq. Cryst.* **6**, 167 (1989).
- [16] M. R. Dodge and C. Rosenblatt, *Phys. Rev. E* **62**, 6891 (2000).
- [17] Y. Lansac, M. A. Glaser, N. A. Clark, and O. D. Lavrentovich, *Nature (London)* **398**, 54 (1999).
- [18] M. Kimura, D. Kang, and C. Rosenblatt, *Phys. Rev. E* **60**, 1867 (1999).